

# Interferometry in dissipative media: Addressing the shallow sea problem for Seabed Logging applications

Evert Slob\* and Kees Wapenaar, Department of Geotechnology, Delft University of Technology

Roel Snieder, Center for Wave Phenomena and Department of Geophysics, Colorado School of Mines

## SUMMARY

We derive interferometric field representations that are valid for diffusive field methods. The method retrieves the reflection response of the earth, as if the domain above the receiver depth level is homogeneous. It is represented as the flux-normalized up going field deconvolved by the down going field. The deconvolution step can be seen as a weighted crosscorrelation step, which is the usual operation in interferometric methods. Because the method effectively redatums the source depth level to the receiver depth level and removes the overburden effects, the shallow sea problem that exists for frequency domain Seabed Logging applications is solved in theory.

## INTRODUCTION

Interferometry is the branch of science that deals with the creation of new field responses by crosscorrelating observations at different receiver locations. Since its introduction in exploration seismology around the turn of the century, the literature on seismic interferometry has grown spectacularly. Many interferometric methods have been developed for random fields and for controlled-source data. The underlying theories have in common that the medium is assumed to be lossless and non-moving, see e.g. the supplement of the 2006 July-August issue of Geophysics. The main reason for this underlying assumption is that the wave equation in lossless and non-moving media is invariant for time-reversal.

Until 2005 it was commonly thought that time-reversal invariance was a necessary condition for interferometry, but recent research shows that this assumption can be relaxed. Slob et al. (2006) analyzed the interferometric method for ground penetrating radar data (GPR), in which losses play a prominent role. They showed that losses lead to amplitude errors as well as the occurrence of spurious events. By choosing the recording locations in a specific way, the spurious events arrive before the first desired arrival and can thus be identified (Slob et al., 2007). By choosing one receiver in a lossless medium, e.g. air, and a configuration with all dissipative parameters outside the surface distribution of noise or transient sources, crosscorrelation methods work without spurious events and amplitude errors in the time window of interest (Slob and Wapenaar, 2007). This approach holds for waves and diffusive fields in dissipative media. Snieder (2006) showed that a volume distribution of uncorrelated noise sources, with source strengths proportional to the dissipation parameters of the medium, precisely compensates for the energy losses (Snieder, R. 2007, Extracting the Greens function of attenuating media from uncorrelated waves, JASA, accepted). As a consequence, the responses obtained by interferometry in such configurations are error free. Also this approach holds for waves in dissipative media and for pure diffusion processes.

Recently we showed that interferometry, including its extensions for waves and diffusion in dissipative and/or moving media, can be represented in a unified form (Wapenaar et al., 2006; Snieder et al., 2007). These representations can also be used for more exotic applications like electroseismic prospecting and quantum mechanics. We have loosened the definition of interferometry to also include crossconvolution methods. Slob et al. (2007) introduce interferometry by crossconvolution and show that it is valid for arbitrary dissipative media. The crossconvolution method does not require a volume distribution of sources, but a restriction is that it only works for transient signals in specific configurations with receivers at opposite sides of the

source array. From these observations we conclude that none of the above described methods provides a practical approach to controlled source electromagnetic (CSEM) applications. Here we demonstrate that ‘interferometry-by-deconvolution’ is applicable in CSEM or in any other exploration method employing diffusion processes. Hence we further loosen the definition of interferometry to also include deconvolution methods, which is particularly useful for Seabed Logging methods.

## INTERFEROMETRY IN DISSIPATIVE MEDIA

The 1D version of interferometry-by-deconvolution was introduced by Riley and Claerbout (1976). It relies on the decomposition of a field at a particular depth level into flux-normalized down going and up going parts. To facilitate such decomposition we employ the reciprocity theorem for one-way fields and apply it on a domain with two horizontal boundaries, see Figure 1. The necessity of flat horizontal boundaries can be relaxed under certain conditions and the derived representations also hold for smoothly curved boundaries (Frijlink, M. and K. Wapenaar, 2007, Reciprocity theorems for one-way wave fields in curvilinear coordinate systems, JASA, submitted). Following Wapenaar and Grimbergen (1996) we write the frequency domain one-way field reciprocity theorem for two independent states  $A$  and  $B$  as,

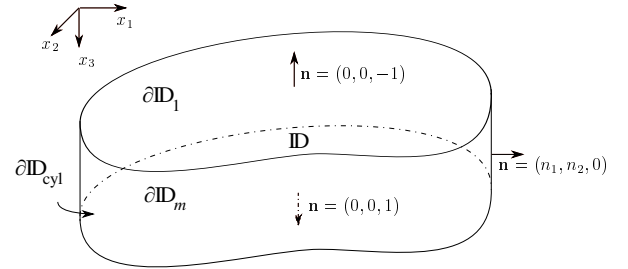


Figure 1: Configuration for one-way reciprocity theorems.

$$\int_{\partial\mathbb{D}} n_3 (\hat{\mathbf{p}}_A)^t \mathbf{N} \hat{\mathbf{p}}_B d^2\mathbf{x} = \int_{\mathbb{D}} \{ (\hat{\mathbf{p}}_A)^t \mathbf{N} \hat{\mathbf{s}}_B + (\hat{\mathbf{s}}_A)^t \mathbf{N} \hat{\mathbf{p}}_B \} d^3\mathbf{x}, \quad (1)$$

where  $\partial\mathbb{D}$  denotes the two flat boundaries with outward unit normal  $n_3$  and the superscript  $t$  denotes transposition. The  $4 \times 1$  electromagnetic field vector  $\mathbf{p}$  contains flux-normalized down and up going fields  $\hat{\mathbf{p}} = (\hat{\mathbf{p}}^+, \hat{\mathbf{p}}^-)^t$  and the  $4 \times 1$  electromagnetic source vector contains flux-normalized down and up going source components  $\hat{\mathbf{s}} = (\hat{\mathbf{s}}^+, \hat{\mathbf{s}}^-)^t$ , given by  $\hat{\mathbf{p}}^\pm = \hat{\mathbf{p}}^\pm(\mathbf{x}, \omega)$  and  $\hat{\mathbf{s}}^\pm = \hat{\mathbf{s}}^\pm(\mathbf{x}, \omega)$  (Reid, 1972; Ursin, 1983). The matrix  $\mathbf{N}$  is given by

$$\mathbf{N} = \begin{pmatrix} \mathbf{0} & \mathbf{I} \\ -\mathbf{I} & \mathbf{0} \end{pmatrix}, \quad (2)$$

the matrices  $\mathbf{I}$  and  $\mathbf{0}$  being the  $2 \times 2$  identity and null matrices, respectively. To construct the vector  $\hat{\mathbf{p}}$  we must record all horizontal components of the electric and magnetic field strengths on a grid and we apply decomposition to these components. Note that equation (1) holds for equal media in the two states inside  $\mathbb{D}$ , while outside  $\mathbb{D}$  the media in the two states can be different. No derivatives occur because we use flux-normalized field quantities.

## Interferometry in dissipative media: Addressing the shallow sea problem for Seabed Logging applications

First we assume that in both states the sources are outside  $\mathbb{D}$ , this reduces equation (1) to

$$\int_{\partial\mathbb{D}_1} \{(\hat{\mathbf{p}}_A^+)^\dagger \hat{\mathbf{p}}_B^- - (\hat{\mathbf{p}}_A^-)^\dagger \hat{\mathbf{p}}_B^+\} d^2\mathbf{x} = \int_{\partial\mathbb{D}_m} \{(\hat{\mathbf{p}}_A^+)^\dagger \hat{\mathbf{p}}_B^- - (\hat{\mathbf{p}}_A^-)^\dagger \hat{\mathbf{p}}_B^+\} d^2\mathbf{x}. \quad (3)$$

In the following analysis state  $B$  represents the actual state of the measured response of the real earth. Consider the marine CSEM acquisition geometry with a sea surface at level  $\partial\mathbb{D}_0$ , see Figure 2(a), with a source at  $\mathbf{x}_S$  in the water layer and the receivers  $\mathbf{x}$  at the bottom of the sea at level  $\partial\mathbb{D}_1$ . Both the water layer and the domain between  $\partial\mathbb{D}_1$  and  $\partial\mathbb{D}_m$  can be heterogeneous. For each source component and after decomposition we have for state  $B$  the down going and up going components of the recorded earth response, given by

$$\mathbf{x} \in \partial\mathbb{D}_1 \quad \begin{cases} \hat{\mathbf{p}}_B^+(\mathbf{x}, \omega) = \hat{\mathbf{p}}^+(\mathbf{x}, \mathbf{x}_S, \omega), \\ \hat{\mathbf{p}}_B^-(\mathbf{x}, \omega) = \hat{\mathbf{p}}^-(\mathbf{x}, \mathbf{x}_S, \omega). \end{cases} \quad (4)$$

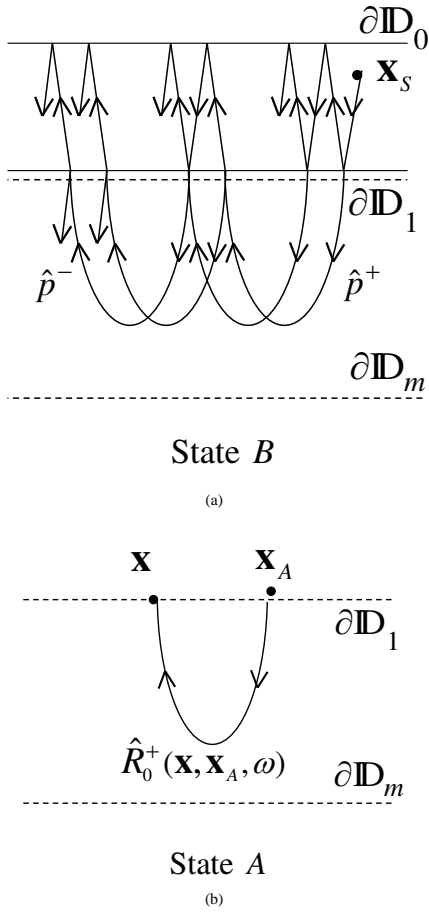


Figure 2: (a) State B: the measured response of the real earth. (b) State A: the response of the medium inside  $\mathbb{D}$  with a homogeneous upper half space, above  $\partial\mathbb{D}_1$ . Both states have a homogeneous lower half space, below  $\partial\mathbb{D}_m$ .

We choose the level  $\partial\mathbb{D}_m$  to be below all heterogeneities, hence there are only non-zero down going field components at the level  $\partial\mathbb{D}_m$ ,

$$\mathbf{x} \in \partial\mathbb{D}_m \quad \begin{cases} \hat{\mathbf{p}}_B^+(\mathbf{x}, \omega) = \hat{\mathbf{p}}^+(\mathbf{x}, \mathbf{x}_S, \omega), \\ \hat{\mathbf{p}}_B^-(\mathbf{x}, \omega) = 0. \end{cases} \quad (5)$$

State  $A$  represents the desired reflection response with a redatumed source at the receiver level of state  $B$  in an earth with different boundary conditions than the real earth, obtained through interferometry-by-deconvolution. The difference is that the medium above the boundary  $\partial\mathbb{D}_1$  is homogeneous and has the same properties as just below  $\partial\mathbb{D}_1$ , see Figure 2(b). For state  $A$  we choose a down going source component just above the level  $\partial\mathbb{D}_1$  and put receivers at the same level  $\partial\mathbb{D}_1$ . We define the reflection response of the medium below  $\partial\mathbb{D}_1$  as the  $2 \times 2$  matrix  $\hat{\mathbf{R}}_0^+(\mathbf{x}, \mathbf{x}_A, \omega)$ , where the subscript '0' denotes that no reflectors exist above  $\partial\mathbb{D}_1$  and the superscript '+' indicates the reflection is a response to a down going source field. We therefore find in state  $A$

$$\mathbf{x} \in \partial\mathbb{D}_1 \quad \begin{cases} \hat{\mathbf{p}}_A^+(\mathbf{x}, \omega) = \begin{pmatrix} \delta(\mathbf{x}_H - \mathbf{x}_{H,A}) & 0 \\ 0 & \delta(\mathbf{x}_H - \mathbf{x}_{H,A}) \end{pmatrix}, \\ \hat{\mathbf{p}}_A^-(\mathbf{x}, \omega) = \hat{\mathbf{R}}_0^+(\mathbf{x}, \mathbf{x}_A, \omega), \end{cases} \quad (6)$$

where the subscript  $H$  is used to denote the horizontal coordinates only, hence  $\mathbf{x}_H = (x_1, x_2)$  and  $\mathbf{x}_{H,A} = (x_{1,A}, x_{2,A})$  (the latter denoting the horizontal coordinates of  $\mathbf{x}_A$ ). At  $\mathbf{x} \in \partial\mathbb{D}_m$  we have again only down going fields,

$$\mathbf{x} \in \partial\mathbb{D}_m \quad \begin{cases} \hat{\mathbf{p}}_A^+(\mathbf{x}, \omega) = \hat{\mathbf{T}}^+(\mathbf{x}, \mathbf{x}_A, \omega), \\ \hat{\mathbf{p}}_A^-(\mathbf{x}, \omega) = \mathbf{0}, \end{cases} \quad (7)$$

where  $\hat{\mathbf{T}}^+(\mathbf{x}, \mathbf{x}_A, \omega)$  is the  $2 \times 2$  transmission response between the levels  $\partial\mathbb{D}_1$  and  $\partial\mathbb{D}_m$ .

Substitution of equations (4)-(7) into equation (3) and using source-receiver reciprocity, i.e.  $\hat{\mathbf{R}}_0^+(\mathbf{x}, \mathbf{x}_A, \omega) = (\hat{\mathbf{R}}_0^+)^\dagger(\mathbf{x}_A, \mathbf{x}, \omega)$ , yields

$$\hat{\mathbf{P}}^-(\mathbf{x}_A, \mathbf{x}_S, \omega) = \int_{\mathbf{x} \in \partial\mathbb{D}_1} \hat{\mathbf{R}}_0^+(\mathbf{x}_A, \mathbf{x}, \omega) \hat{\mathbf{P}}^+(\mathbf{x}, \mathbf{x}_S, \omega) d^2\mathbf{x}, \quad (8)$$

where the up and down going responses,  $\hat{\mathbf{P}}^-$ ,  $\hat{\mathbf{P}}^+$ , are now  $2 \times 2$  matrices because we have two source components. Equation (8) is a Fredholm integral equation of the first kind in the reflection coefficient matrix  $\hat{\mathbf{R}}_0^+(\mathbf{x}_A, \mathbf{x}, \omega)$ . The reflection coefficient matrix is the retrievable flux-normalized Green's function, representing the impulse response at a receiver location  $\mathbf{x}_A \in \partial\mathbb{D}_1$  due to a down going source component at position  $\mathbf{x} \in \partial\mathbb{D}_1$ . For laterally invariant media it can easily be solved by simple  $2 \times 2$  matrix inversion for each wavenumber-frequency component separately. Of course this requires two independent source components. For general 3D heterogeneous media it can only be solved when the decomposed data,  $\hat{\mathbf{P}}^-(\mathbf{x}_A, \mathbf{x}_S, \omega)$  and  $\hat{\mathbf{P}}^+(\mathbf{x}, \mathbf{x}_S, \omega)$  is recorded at a sufficient number of receiver positions  $\mathbf{x}_A \in \partial\mathbb{D}_1$  and for a sufficient number of source positions  $\mathbf{x}_S$ . It follows that two horizontal source electric dipole orientations are sufficient to solve equation (8) uniquely, see e.g. Holvik and Amundsen (2005) for an elastic example. In matrix notation (Berkhout, 1982), equation (8) can be written as

$$\hat{\mathbf{P}}^- = \hat{\mathbf{R}}_0^+ \hat{\mathbf{P}}^+. \quad (9)$$

For example, the columns of matrix  $\hat{\mathbf{P}}^+$  contain both components of  $\hat{\mathbf{p}}^+(\mathbf{x}, \mathbf{x}_S, \omega)$  for fixed  $\mathbf{x}_S$  and variable  $\mathbf{x}$  at  $\partial\mathbb{D}_1$ , whereas the rows of this matrix contain  $\hat{\mathbf{p}}^+(\mathbf{x}, \mathbf{x}_S, \omega)$  for fixed  $\mathbf{x}$  and variable  $\mathbf{x}_S$  and both source components at  $\partial\mathbb{D}_S$ , where  $\partial\mathbb{D}_S$  represents the depth level of the sources. Inversion of equation (9) involves matrix inversion, according to

$$\hat{\mathbf{R}}_0^+ = \hat{\mathbf{P}}^-(\hat{\mathbf{P}}^+)^{-1} \quad (10)$$

(Wapenaar K. and D.J. Verschuur, 1996, Processing of ocean bottom data: The Dolphin Project, Volume I, p.6.1-6.26). The matrix inversion in equation (10) can be stabilized by least-squares inversion, according to

$$\hat{\mathbf{R}}_0^+ = \hat{\mathbf{P}}^-(\hat{\mathbf{P}}^+)^{\dagger} [\hat{\mathbf{P}}^+(\hat{\mathbf{P}}^+)^{\dagger} + \varepsilon^2 \mathbf{I}]^{-1}, \quad (11)$$

where the superscript  $\dagger$  denotes transposition and complex conjugation,  $\mathbf{I}$  is the identity matrix and  $\varepsilon$  is a small constant. Berkhout and

## Interferometry in dissipative media: Addressing the shallow sea problem for Seabed Logging applications

Verschuur (2003) used a similar inversion for transforming surface-related multiples into primaries. Equations (10) and (11) describe 3D interferometry-by-deconvolution and is similar to the least squares re-adding method described by Schuster and Zhou (2006). When we ignore the inverse matrix in equation (11) we arrive at

$$\hat{R}_0^+ \approx \hat{P}^-(\hat{P}^+)^{\dagger}. \quad (12)$$

which is the matrix form expression in the frequency domain of Bakulin and Calvert's virtual source method (Bakulin and Calvert, 2006). Of course in our case the matrix  $\hat{P}^+(\hat{P}^+)^{\dagger}$  is not close to I and equation (12) cannot be used for CSEM data. Comparing equation (12) with equation (11) it can be seen that the here proposed method of interferometry by deconvolution is a weighted form of the usual cross-correlation method, with the inverse matrix in equation (11) as the weight.

### NUMERICAL EXAMPLES

To illustrate interferometry-by-deconvolution with a numerical example, we apply it to simulated 2D CSEM data as a simple demonstration of the advantage of this method for hydrocarbon exploration with the Seabed Logging method. Amundsen et al. (2006) showed already that decomposition of CSEM data into down going and up going fields improves the detectability of hydrocarbon reservoirs. Here we show that the combination of decomposition followed by interferometry-by-deconvolution not only improves the detectability but also results in improved quantitative information about the reservoir parameters.

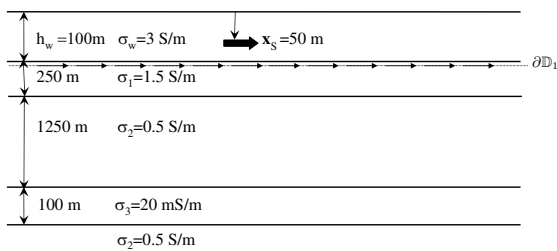


Figure 3: Configuration for the 2D example for Seabed Logging applications.

The model consists of a plane layered Earth and the TM-mode configuration is used, which is the proper two-dimensional approximation of the CSEM method as applied in Seabed Logging applications with an in-line horizontal electric dipole (HED) and in-line electric field receivers. Since this is a 2D scalar example, the in-line HED is sufficient and only a single source position is needed because we assume a horizontally shift-invariant medium. To allow for decomposition into down going and up going field components, we record the in-line electric field strength and the cross-line magnetic field strength. The model is shown in Figure 3, where the seawater layer contains an in-line electric current source at 50 m above the sea bottom. The receivers are located at the sea bottom with a total extent of 40 km. The water layer is modeled with a thickness of 100 m as a model for a shallow sea. The seawater has a conductivity of  $\sigma_w=3$  S/m. Below the sea bottom there is a layer with a conductivity of  $\sigma_1=1.5$  S/m with a thickness of 250 m. This is followed by a half-space with  $\sigma_2=0.5$  S/m, which is intersected after 1250 m by a reservoir-type layer with a thickness of 100 m and a conductivity of  $\sigma_3=50$  mS/m. Note that the top of this reservoir layer is located at 1500 m below the sea bottom. To compare with a signal strength in the same background medium without reservoir layer, we also model the response of the background medium. The source frequency is taken at  $f_s = 0.5$  Hz. All plots show the responses

in presence of the reservoir layer in solid red-lines and the responses in absence of the reservoir layer in dashed blue lines. We use a linear offset scale and a ten-base logarithmic amplitude scale for all figures showing responses.

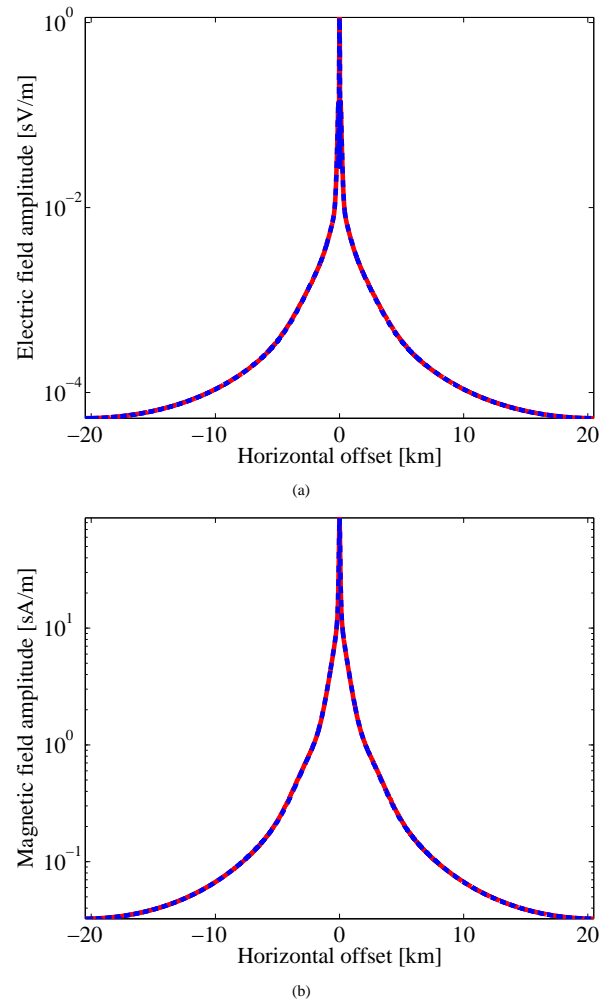
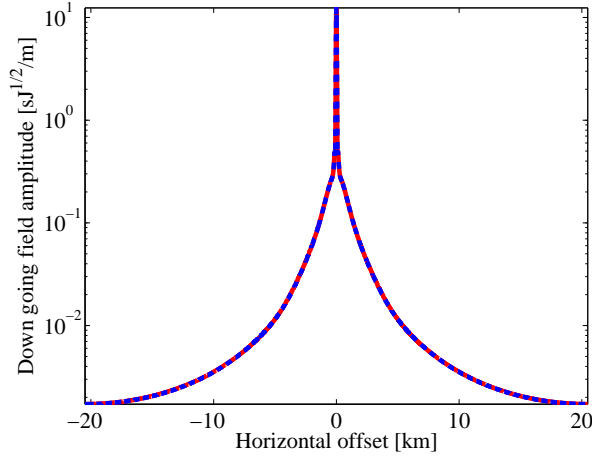


Figure 4: In-line electric field response  $\mathbf{x} \in \partial\mathbb{D}_1$  in presence (solid red curve) and absence (dashed blue curve) of the reservoir at (a); Cross-line magnetic field response at  $\mathbf{x} \in \partial\mathbb{D}_1$  in presence (solid red curve) and absence (dashed blue curve) of the reservoir layer.

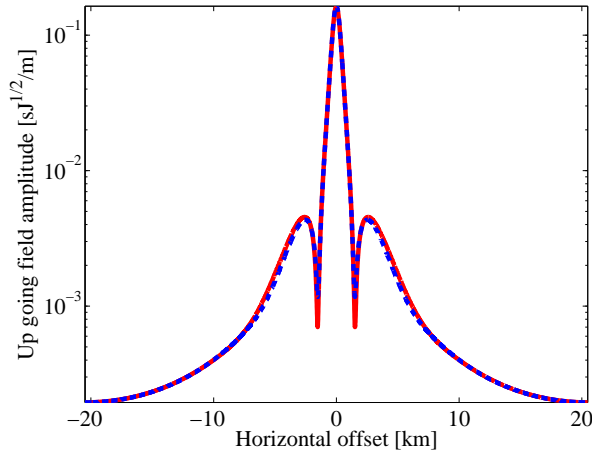
Figure 4(a) shows the recorded in-line component of the electric field at the bottom of the sea, while Figure 4(b) shows the recorded cross-line component of the magnetic field at the bottom of the sea. From both figures it can be seen that the presence of the reservoir layer is not visible in the plots because the red and blue curves almost completely overlap. As a first step in our interferometry-by-deconvolution procedure we carry out the decomposition of the recorded field components into down going and up going flux-normalized field components with the medium parameters of the layer just below the sea bottom and hence they correspond to the fields that would have been measured when they were positioned just below the sea bottom. They are shown in Figures 5(a) and 5(b), respectively. It is clear from these figures that the up going field is more than ten times smaller in amplitude than the down going field. In Figure 5(a) it can be seen that the blue curve masks the red curve for all offsets, indicating that the presence of the reservoir layer is not visible in the down going field part just as in the total field. As can be seen in Figure 5(b), the up going field shows the

## Interferometry in dissipative media: Addressing the shallow sea problem for Seabed Logging applications

presence of the reservoir layer for offsets between approximately 2.5 km to 7 km. Still the up going field response is strongly influenced by the shallow sea indicating that there is relatively strong interaction with the sea surface and the layer below the sea bottom, which is part of the up going field response.



(a)



(b)

Figure 5: Flux-normalized down going field response,  $\hat{p}^+(\mathbf{x}, \mathbf{x}_S, \omega)$ , just below  $\partial\mathbb{D}_1$  in presence (solid red curve) and absence (dashed blue curve) of the reservoir layer (a); Flux-normalized up going field response,  $\hat{p}^-(\mathbf{x}_A, \mathbf{x}_S, \omega)$ , just below  $\partial\mathbb{D}_1$  in presence (solid red curve) and absence (dashed blue curve) of the reservoir layer.

Removing the effect of the water layer from the up going field by deconvolving it with the down going field results in a much clearer reflection response as can be seen in Figure 6, where from offsets of approximately 2 km onward the presence of the reservoir is clearly visible. An other important aspect is the absence of amplitude saturation for large offsets when the water layer has been removed, as can be seen by comparing the amplitude behavior of the up going field in Figure 5(b) and the retrieved reflection response in Figure 6 where the amplitude continues to decrease with increasing offset. Obviously, this continuing decrease in amplitude requires high precision data, finite recording precision and noise will prevent practical applications at very large offsets. However, there is clearly a practical offset range where it will work on actual measured data. In our example model the effect of the first layer of 250 m thickness still has a major effect on the deconvolved reflection response at near offsets because the lower half space in the embedding has a much lower electric conductivity

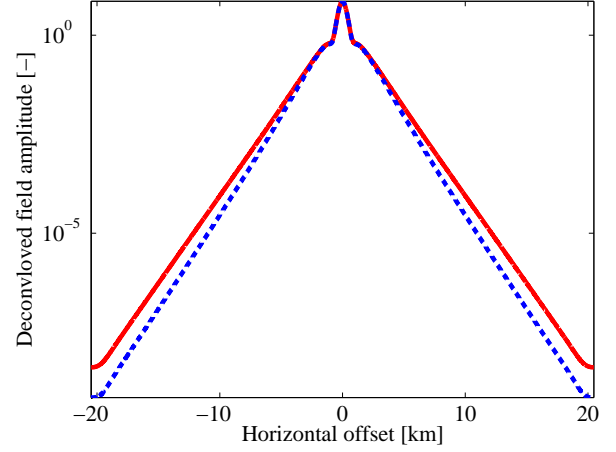


Figure 6: Subsurface reflection response,  $\hat{R}_0^+(\mathbf{x}_A, \mathbf{x}, \omega)$ , as if the the air and sea layers are absent, obtained by interferometry-by-deconvolution, which response is thus independent of the water depth. The red solid line and blue dashed line are for the situation with and without the reservoir layer, respectively.

than the first layer. The contrast is a factor 3 at a vertical distance of 250 m below the receivers, while the contrast of the reservoir with its surroundings is a factor 10 at 1500 m below the receivers. It can be understood that for deeper receivers, e.g. placed in a horizontal well, the proposed method can result in removal of these near sea bottom, high conductivity layers and produce an even cleaner reflection response of the target.

## CONCLUSIONS

We have formulated an interferometric method using the deconvolution concept to create new responses using recorded responses that are valid and practical for CSEM as applied in the Seabed Logging method. This is an extension of known interferometric methods that use the lossless medium assumption. The method is developed into an algorithm that can be used on data from Seabed Logging or from other electromagnetic recordings at the bottom of the sea or in a (horizontal) borehole. The algorithm requires sufficient number of source components (for 3D data) and source positions. These source positions can be on the earth surface for land methods or in the sea for Seabed Logging methods, either transient or with only a limited number of frequencies. The developed algorithm not only moves the source to the receiver depth level ('source redatuming'), but also removes all overburden effects of heterogeneities above the receiver depth level (changed boundary conditions). The result is a reflection response that is obtained from positions closer to the target and without disturbing overburden effects. As in all interferometric methods, no information about the medium properties is required.

Removing the overburden effect effectively solves the shallow sea problems in frequency domain Seabed Logging methods, while for possible deep receivers our proposed method will remove all overburden effects and produce a clean target reflection response.

## ACKNOWLEDGMENTS

This work is supported by the Netherlands Research Centre for Integrated Solid Earth Science (ISES) and the sponsors of the CWP project.

## Interferometry in dissipative media: Addressing the shallow sea problem for Seabed Logging applications

### REFERENCES

- Amundsen, L., L. Løseth, R. Mittet, S. Ellingsrud, and B. Ursin, 2006, Decomposition of electromagnetic fields into upgoing and downgoing components: *Geophysics*, **71**, G211–G223.
- Bakulin, A. and R. Calvert, 2006, The virtual source method: Theory and case study: *Geophysics*, **71**, S1139–S1150.
- Berkhout, A., 1982, *Seismic Migration, Imaging of acoustic energy by wavefield extrapolation*: Elsevier.
- Berkhout, A. and D. Verschuur, 2003, Transformation of multiples into primaries: 73rd Annual Internat. Mtg. Soc. Expl. Geophys., Expanded Abstracts, 1925–1928.
- Holvik, E. and L. Amundsen, 2005, Elimination of the overburden response from multicomponent source and receiver seismic data, with source designation and decomposition in PP-, PS-, SP- and SS-wave responses: *Geophysics*, **70**, S111–S121.
- Reid, W., 1972, *Riccati differential equations*: Academic Press.
- Riley, D. and J. Claerbout, 1976, 2-D multiple reflections: *Geophysics*, **41**, 592–620.
- Schuster, G. and M. Zhou, 2006, A theoretical overview of model-based and correlation-based redatuming methods: *Geophysics*, **71**, S1103–S1110.
- Slob, E., D. Draganov, and K. Wapenaar, 2006, GPR without a source: The 11th International Conf. on GPR, Expanded Abstracts, Ant.6.
- , 2007, Interferometric electromagnetic green's functions representations using propagation invariants: *Geoph. J. Int.*, **169**, 60–80, doi:10.1111/j.1365-246X.2006.03296.x.
- Slob, E. and K. Wapenaar, 2007, Electromagnetic Greens functions retrieval by cross-correlation and cross-convolution in media with losses: *Geoph. Res. Lett.*, **34**, L05307, doi:10.1029/2006GL029097.
- Snieder, R., 2006, Retrieving the Green's function of the diffusion equation from the response to a random forcing: *Phys. Rev. E.*, **74**, 046620–1–046620–4, doi:10.1103/PhysRevE.74.046620.
- Snieder, R., K. Wapenaar, and U. Wegler, 2007, Unified Green's function retrieval by cross-correlation; connection with energy principles: *Phys. Rev. E*, **75**, 0361103–1–036103–14.
- Ursin, B., 1983, Review of elastic and electromagnetic wave propagation in horizontally layered media: *Geophysics*, **48**, 1063–1081.
- Wapenaar, C. and J. Grimbergen, 1996, Reciprocity for one-way wave equations: *Geophys. J. Int.*, **127**, 169–177.
- Wapenaar, K., E. Slob, and R. Snieder, 2006, Unified Greens Function Retrieval by Cross Correlation: *Phys. Rev. Lett.*, **97**, 234301–1–4, doi:10.1103/PhysRevLett.97.234301.